Modeling and Control for Lateral Rail Vehicle Dynamic Vibration with Comfort Evaluation

Mortadha Graa, Mohamed Nejlaoui, Ajmi Houidi, Zouhaier Affi and Lotfi Romdhane

Abstract Investigation of vibration is an important topic for the purposes of ride Investigation of control vibration is an important topic for the purposes of ride comfort in railway engineering. The vibration of rail vehicles becomes very complex because it is affected by the condition of vehicles, including suspensions and wheel profile, condition of track sections, including rail profile, rail irregularities, cant and curvature. The present study deals with the modeling and control for lateral rail vehicle active suspension by PID-ZN controller. For this, a numerical simulation of the dynamic behavior is made based on the Lagrangian approach in order to study the effect of vehicle speed in response to imperfections in the tracks. A model of 17 degrees of freedom is adopted which consists of one car body 2 bogies and 4 wheel-sets. A Sperling ride index (ISO2631) is calculated using filtered RMS accelerations in order to evaluate the ride comfort. Which allowing at the same time the evaluation of the dynamic behavior of the car body and the level of passenger comfort by analyzing the accelerations at the center of mass of the car body.

Keywords ISO 2631 · Active suspension · Passive suspension · PID controller · Comfort dynamic behavior · Ride comfort · Lateral dynamic vibration

M. Graa (✉) · M. Nejlaoui · Z. Affi
Laboratoire de Génie Mécanique (LGM), Ecole Nationale d'Ingénieurs de Monastir, Université de Monastir, Monastir, Tunisia
e-mail: graa_mortadha@yahoo.fr

A. Houidi · L. Romdhane
Laboratoire de Mécanique de Sousse (LMS), Ecole Nationale d'Ingénieurs de Sousse, Université de Sousse, Sousse, Tunisia

L. Romdhane
College of Engineering, American University of Sharjah, Sharjah, United Arab Emirates

T. Fakhfakh et al. (eds.), *Advances in Acoustics and Vibration*,
Applied Condition Monitoring 5, DOI 10.1007/978-3-319-41459-1_9

1 Introduction

Rail comfort is one of the priority axes of the designers of rail vehicles. However, the comfort that passengers experience is usually perceived differently from one individual to another. Proved in several research works, track defects present the main sources noise and vibration for the rail vehicles. The nature of vibration itself is random and covers a wide frequency range (Skarlatos et al. 2004). The improvement of the passenger comfort while travelling has been the subject of intense interest for many train manufacturers, researchers and companies all over the world. Although new techniques in manufacturing and design ensure better ride quality in railway carriages, it is sometimes impossible to completely eliminate track defects or various ground irregularities. This comfort is highly affected by the vehicle speed and the rail imperfections. Improving the rail vehicle suspension is the key to avoid high perturbations, to be transmitted from the wheels to the passenger. The classical passive suspensions are able to absorb only a limited part of these perturbations dynamic behavior of the car body comfort in a more efficient way.

Several studies have been performed on rail vehicle with passive suspensions. Nejlaoui et al. (2013) optimized the structural design of passive suspensions in order to ensure simultaneously passenger safety and comfort. Abood and Khan (2011) investigated the Railway carriage simulation model to study the influence of vertical secondary suspension stiffness on ride comfort of railway car body. Zhang et al. (2013) developed a finite elements optimization technique to find the best parameters of the passive suspension in order to improve the train riding comfort. The objective is to reach the best compromise between the ride quality and the suspension deflections.

Other works focused on the study of active suspension systems where a controlled actuator is embedded in the system. Zhou et al. (2010) developed an active lateral secondary suspension of railway vehicles in order to attenuate the vehicle body lateral vibration. This active suspension is controlled by the use of skyhook dampers. To decrease the effect of road vibration problems, Eski and Yıldırım (2009) controlled the vibration of the vehicle suspension by using a PID controller. The LQR method was also used in designing active suspensions (Pratt 2002; Vincent 1999).

Safety and comfort are evaluated with specific performance indices. To inspect the motion within the range of human comfort, a Sperling's ride index is measured for the ride comfort ISO 2631 (Kumar 2006). There exists complex dynamics between the rail and wheel. In fact, an accuracy modeling of the rail vehicle dynamics is often difficult. In the physical system, the input comes from the actual track. In a model, the user-defined input can be created analytically or can be based on actual measurements. For this study analytic track data are created using mathematical shapes, to represent the track geometry (Dukkipati and Amyot 1988).

2 Modeling of Rail Road Vehicle

To analyze the dynamic behavior of railway vehicles, usually the vehicle (and if necessary the environment) is represented as a multi body system. A multi body system consists of rigid bodies, interconnected via massless force elements and joints. Due to the relative motion of the system's bodies, the force elements generate applied forces and torques. Typical examples of such force elements are springs, dampers, and actuators combined in primary and secondary suspensions of railway vehicles.

2.1 Assumptions

The assumptions made in formulating the model are as follows:

- Bogie and car body component masses are rigid.
- The springs and dampers of the suspension system elements have linear characteristics.
- Friction does not exist between the axle and the bearing.
- The vehicle is moving with constant velocity on a rigid and constant gauge.
- All wheel profiles are identical from left to right on a given axle and from axle to axle and all wheel remain in contact with the rails.
- Straight track.
- An irregularity in the vertical direction with the same shape for left and right rails.

2.2 Rail Road Vehicle Model

Figure 1 illustrates the train vehicle model adopted in this study. It consists of a vehicle body, two bogies frames and four wheel-sets. Each bogie consists of the bogie frame, and two wheel sets. The car body is modeled as a rigid body having a mass M_c; and having moment of inertia J_{bx} and J_{cz} about the longitudinal and vertical axes, respectively. Similarly, each bogie frame is considered as a rigid body with a mass m_b (m_{b1} and $_{mb2}$) with moment of inertia J_{bx} and J_{bz} about the longitudinal and vertical axes, respectively. Each axle along with the wheel set has a mass m_w (for four axles m_{w1}; m_{w2}; m_{w3} and m_{w4}). The spring and the shock absorber in the primary suspension for each axle are characterized by a spring stiffness K_p and a damping coefficient C_p, respectively. Likewise, the secondary suspension is characterized by spring stiffness K_s and damping coefficient C_s, respectively. As the vehicle car body is assumed to be rigid, its motion may be described by the lateral displacement and rotations about the vertical axis (yaw or Ψ_c) and about the

longitudinal axis (roll or θ_c). Similarly, the movements of the two bogies units are described by three degrees of freedom y_{bi}; Ψ_{bi} and θ_{bi} (i = 1, 2), each about their centers. Each axle set is described by two degrees of freedom y_w; and Ψ_w. about their centers. Totally, 17 degrees of freedom have been considered in this study for the vehicle model shown in Fig. 1. The detailed parameters regarding the moment of inertia and mass of different component are given in Table 1.

Some parameters regarding the rigid bodies are already given in Table 1; however, the other parameters, which are essential for the simulation of the vehicle, are presented in Table 2. A typical rail road vehicle system is composed of various components such as car body, springs, dampers, Bogies, Wheel-set, and so forth.

When such dynamic systems are put together from these components, one must interconnect rotating and translating inertial elements with axial and rotational springs and dampers, and also appropriately account for the kinematics of the system structure.

To minimize the car body vibrations, tow lateral actuators are designed: one controller actuator per bogie in a vehicle (Fig. 1). The lateral controllers are designed to suppress car body lateral, yaw and roll angular vibrations caused by lateral rail disturbances.

The control force vector can be given as: $(i = 1, 2, j = 1 \ldots 4)$

$$[\boldsymbol{F}_u] = \left[\boldsymbol{F}_c^u \;\; \boldsymbol{F}_{bi}^u \;\; \boldsymbol{F}_{wj}^u\right] \tag{1}$$

where $\boldsymbol{F}_c^u$, $\boldsymbol{F}_{bi}^u$ and $\boldsymbol{F}_{wj}^u$ are the car body, bogie i and wheel-set j control forces, respectively, given in following:

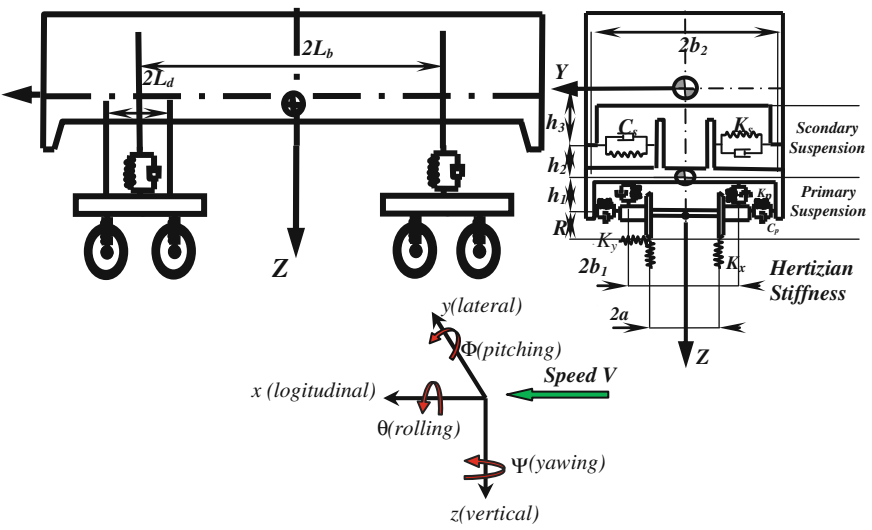

Fig. 1 Physical model of railway vehicle

Table 1 Detailed parameter of rigid bodies

Name of rigid bodies	Mass (kg)	Moment of inertia (kg m^2)	
		I_{XX}	I_{ZZ}
Car body	6.7×10^5	10^5	10^6
Bogie-I and II	10^5	10^5	10^5
Wheel-set-I, II, III and IV	4000	4000	4000

Table 2 Vehicle parameters

Parameter	Nomenclature	Values
Primary spring stiffness	K_p	10^6 N/m
Secondary spring stiffness	K_s	1.7×10^6 N/m
Primary damping coefficient	C_p	6×10^4 Ns/m
Secondary damping coefficient	C_s	10^5 Ns/m
Lateral hertz spring stiffness	K_{hz}	35×10^9 N/m
Longitudinal distance between bogies I and II and car body mass center	L_b	6 m
Longitudinal distance between wheel-set and corresponding bogie origin	L_d	1.4 m
Lateral distance between a longitudinal primary suspension and corresponding wheel-set	d_p	1 m
Lateral distance between longitudinal secondary suspension and corresponding bogie origin	d_s	1 m
Lateral distance between contact point of wheel–rail and corresponding wheel-set origin	a	0.7163 m
Lateral distance between vertical primary suspension and corresponding wheel-set origin	b_1	1 m
Lateral distance between vertical secondary suspension and car body mass center	b_2	1 m
Nominal wheel radius	R_1	0.61 m
Vertical distance between wheel-set and bogie mass centers	h_1	0.3 m
Vertical distance between bogie mass center and lateral secondary suspension	h_2	0.2 m
Vertical distance between lateral secondary suspension and car body mass center	h_3	1.3 m

$$\boldsymbol{F}_{\boldsymbol{c}}^{\boldsymbol{u}} = \begin{bmatrix} \sum_{\mathrm{i}=1}^{2} u_{\mathrm{yi}} \\ h_3 \sum_{\mathrm{i}=1}^{2} u_{\mathrm{yi}} \\ L_b \left[u_{\mathrm{y1}} - u_{\mathrm{y3}} \right] \end{bmatrix}^T \tag{2}$$

$$\boldsymbol{F}_{\boldsymbol{ti}}^{\boldsymbol{u}} = \begin{bmatrix} -u_{\mathrm{yi}} & h_2 u_{\mathrm{yi}} & 0 \end{bmatrix} \tag{3}$$

$$\boldsymbol{F}_{\boldsymbol{wj}}^{\boldsymbol{u}} = [0 \quad 0 \quad 0 \quad 0] \tag{4}$$

2.3 Equation of Motion

The equations of motion of the railway vehicle are obtained by means of the Lagrange equation. We obtained the following equations of motion for the wheel-set *j*:

$$\begin{aligned} & m_{wj}\ddot{y}_{wj} + 2C_p\left[-\dot{y}_{bi} + \dot{y}_{wj} - h_1\dot{\theta}_{bi} + (-1)^i L_d\dot{\psi}_{bi}\right] \\ & \quad + 2K_p\left[-y_{bi} + y_{wj} - h_1\theta_{bi} + (-1)^i L_d\psi_{wj}\right] \\ & \quad + k_{hy}\left[y_{wj}\left(1 + R_1\frac{\lambda}{a}\right) - y_{rj}\right] + 2\left[f_{11}\left(\frac{\dot{y}_{wj}}{V} - \psi_{wj}\right) + f_{12}\left(\frac{\dot{\psi}_{wj}}{V}\right)\right] = 0 \end{aligned} \tag{5}$$

$$\begin{aligned} & J_{zwj}\ddot{\psi}_{wj} + 2d_p^2 C_p\left[-\dot{\psi}_{bi} + \dot{\psi}_{wj}\right] + 2d_p^2 K_p\left[-\psi_{bi} + \psi_{wj}\right] \\ & \quad + 2\left[f_{11}\left(\frac{\dot{y}_{wj}}{V} - \psi_{wj}\right) + f_{12}\left(\frac{\dot{\psi}_{wj}}{V}\right)\right] = 0 \end{aligned} \tag{6}$$

where j = 1, 2 when $i = 1$, $j = 3, 4$ when $i = 2$, $k = 1$ when $j = 1$, $k = 3$ when $j = 2$, $k = 5$ when $j = 3$, $k = 7$ when $j = 4$; the dot indicates differentiation with respect to time variable t; f_{11} is the lateral creep coefficient; f_{12} is the lateral/spin creep coefficient.

The equations of motion of the bogie *i* are:

$$\begin{aligned} & m_{bi}\ddot{y}_{bi} + 2C_p\left[2\dot{y}_{bi} - (\dot{y}_{wj} + \dot{y}_{w(j+1)}) + 2h_1\dot{\theta}_{bi}\right] \\ & \quad + 2C_s\left[-\dot{y}_c + \dot{y}_{bi} - (h_3\dot{\theta}_c + h_2\dot{\theta}_{bi}) - kL_b\dot{\psi}_c\right] \\ & \quad + 2K_p\left[2y_{bi} - (y_{wj} + y_{w(j+1)}) + 2h_1\theta_{bi}\right] \\ & \quad + 2K_s\left[-y_c + y_{bi} - (h_3\theta_c + h_2\theta_{bi}) - kL_b\psi_c\right] = -u_{yi} \end{aligned} \tag{7}$$

$$\begin{aligned}
&J_{xbi}\ddot{\theta}_{bi} + 2h_1C_p\left[2h_1\dot{\theta}_{bi} + 2\dot{y}_{bi} - (\dot{y}_{wj} + \dot{y}_{w(j+1)})\right] \\
&\quad + 2h_2C_s\left[h_3\dot{\theta}_c + h_2\dot{\theta}_{bi} + \dot{y}_c - \dot{y}_{bi} + kL_b\dot{\psi}_c\right] \\
&\quad + 2b_1^2C_p\left[2\dot{\theta}_{bi} - \frac{\lambda}{a}\left(\dot{y}_{wj} + \dot{y}_{w(j+1)}\right)\right] + 2b_2^2C_s\left[-\dot{\theta}_{bi} + \dot{\theta}_c\right] \\
&\quad + 2h_1K_p\left[2h_1\theta_{bi} + 2y_{bi} - (y_{wj} + y_{w(j+1)})\right] \\
&\quad + 2h_2K_s[h_3\theta_c + h_2\theta_{bi} + (y_c - y_{bi}) + kL_b\psi_c] \\
&\quad + 2b_1^2K_p\left[2\theta_{bi} - \frac{\lambda}{a}\left(y_{wj} + y_{w(j+1)}\right)\right] + 2b_2^2K_s[\theta_{bi} - \theta_c] = h_2u_{yi}
\end{aligned} \tag{8}$$

$$\begin{aligned}
&J_{zbi}\ddot{\psi}_{bi} + 2d_p^2C_p\left[2\dot{\psi}_{bi} - (\dot{\psi}_{wj} + \dot{\psi}_{w(j+1)})\right] \\
&\quad + 2L_dC_p\left[2L_d\dot{\psi}_{bi} - (\dot{y}_{wj} - \dot{y}_{w(j+1)})\right] \\
&\quad + 2d_p^2K_p\left[2\psi_{bi} - (\psi_{wj} + \psi_{w(j+1)})\right] + 2d_s^2K_s(\psi_{bi} - \psi_c) \\
&\quad + 2L_dK_p\left[2L_d\psi_{bi} - (\psi_{wj} + \psi_{w(j+1)})\right] = 0
\end{aligned} \tag{9}$$

where $j = 1$ and $k = 1$ when $i = 1$; $j = 3$ when $i = 2$; $j = 5$ and $k = -1$ when $i = 3$.

Finally, the equations of motion of the car body are:

$$\begin{aligned}
&m_c\ddot{y}_c + 2C_s\left[2(\dot{y}_c + h_3\dot{\theta}_c) - \sum_{p=1}^{2}\dot{y}_{bp} + h_2\sum_{p=1}^{2}\dot{\theta}_{bp}\right] \\
&\quad + 2K_s\left[2(y_c + h_3\theta_c) - \sum_{p=1}^{2}y_{bp}\right] + h_2(\theta_{b1} + \theta_{b2}) = \sum_{p=1}^{2}u_{yp}
\end{aligned} \tag{10}$$

$$\begin{aligned}
&J_{xc}\ddot{\theta}_c + 2h_3C_s\left[2(h_3\dot{\theta}_c + \dot{y}_c) + h_2\sum_{p=1}^{2}\dot{\theta}_{bp} - \sum_{p=1}^{2}\dot{y}_{bp}\right] + 2b_2^2C_s\left[2\dot{\theta}_c - \sum_{p=1}^{2}\dot{\theta}_{bp}\right] \\
&\quad + 2h_3K_s\left[2(h_3\theta_c + y_c) + h_2\sum_{p=1}^{2}\theta_{bp} - \sum_{p=1}^{2}y_{bp}\right] + 2b_2^2K_s\left[2\theta_c - \sum_{p=1}^{2}\theta_{bp}\right] = h_3\sum_{p=1}^{2}u_{yp}
\end{aligned} \tag{11}$$

$$\begin{aligned}
&J_{zc}\ddot{\psi}_c + 2L_bC_s\left[2L_b\dot{\psi}_c + (-\dot{y}_{b1} + \dot{y}_{b2}) - h_2(-\dot{\theta}_{b1} + \dot{\theta}_{b2})\right] \\
&\quad + \left[2d_s^2\left[\begin{array}{c} K_s(2\psi_c - (\psi_{b1} + \psi_{b2}) + K_s(\psi_c - \psi_{b2}) \\ + 2L_bK_s\left[\begin{array}{c} 2L_b\psi_c + (-y_{b1} + y_{b2}) \\ + h_2(-\theta_{b1} + \theta_{b2}) \end{array}\right] \end{array}\right]\right] = L_b(u_{y1} - u_{y3})
\end{aligned} \tag{12}$$

3 Track Inputs to Rail Road Vehicle

The dynamic wheel loads generated by a moving train are mainly due to various wheel/track imperfections. These imperfections are considered as the primary source of dynamic track input to the railroad vehicles. Normally, the imperfections that exist in the rail-track structure are associated with the vertical and lateral track profile, cross level, rail joint, wheel flatness, wheel/rail surface corrugations and sometimes uneven support of the sleepers.

In actual practice different types of periodic, a-periodic or random track irregularities may exist on the track, but in the present study a lateral local discontinuity type of irregularity is considered as shown in Fig. 2. The shape of the irregularity is assumed to be similar on the left and the right rails.

The excitations of the left wheels of leading bogies are as follows:

$$Y_{ri} = \begin{cases} H & for \quad t_{di} \leq t \\ 0 & otherwise \end{cases} (i = 1..4) \tag{13}$$

where

$$[t_{d1}, t_{d2}, t_{d3}, t_{d4}] = \left[0, \frac{2L_d}{V}, \frac{2L_b}{V}, \frac{2L_b + 2L_d}{V}\right] \tag{14}$$

In the present study, H is taken as 0.03 m.

4 Control Strategies and Design

In this section, the design of the PID controller for improving the ride passenger comfort is presented.

The different controller gains will be determined according to the rail vehicle dynamic. The PID controller block diagram is given in Fig. 3. The objective of the

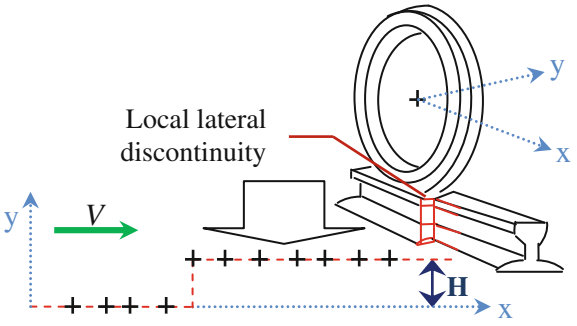

Fig. 2 Model of track irregularity

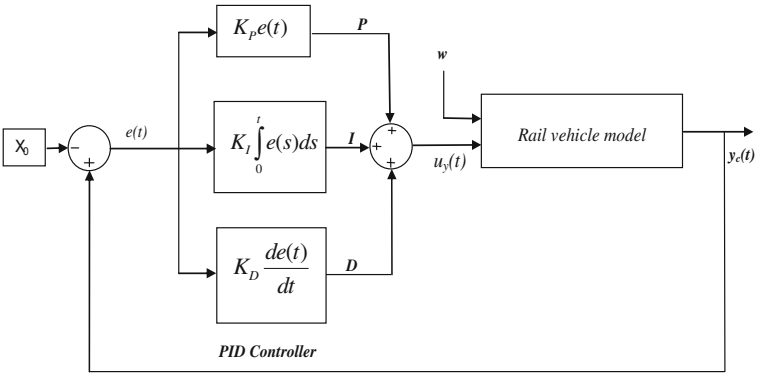

Fig. 3 The block diagram of PID controller

Table 3 PID gains

Lateral control force	K_P	K_D	K_I
U_{yi} (i = 1,2)	121	2432	42,654

PID is to minimize an error e(t) through the control of the active suspension. The output of the PID controller is given by:

$$u_{yi}(t) = K_P e(t) + K_I \int_0^t e(s)ds + K_D \frac{de(t)}{dt} \tag{15}$$

where K_P, K_I and K_D are proportional, integral and derivative gains, respectively.

$u_{yi}(t)$ is the control force.

We will substitute the PID controller and the open loop return with a level step. To find the values of the PID gains, we have used the step response Ziegler-Nichols method (Ang et al. 2005; Wolfgang 2005). Table 3 presents these gains.

5 Simulation and Comfort Evaluation

The models were built in the MATLAB/Simulink® environment. The fixed step solver ODE-45 (Dormand-Prince) was utilized, with the sampling time Ts = 0.0001.

Dynamic analysis was carried out for the vehicle at different speeds: 15, 30, 45 and 60 m/s.

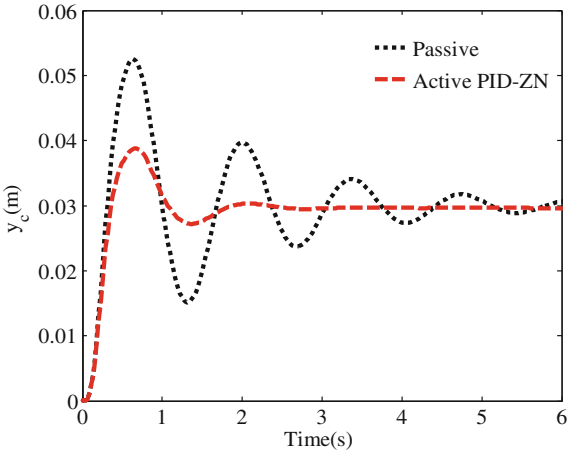

Fig. 4 The lateral Car body displacement for 60 m/s

Table 4 Sperling's ride index evaluation for different vehicle velocities (passive system)

Vehicle speed (m/s)	Sperling index (W_z)	Ride comfort evaluation
15	3.17	Strong, irregular, but still tolerable
30	2.54	More pronounced but not unpleasant
45	2.15	Clearly noticeable
60	2.03	Clearly noticeable

Figure 4 presents the lateral car body displacement for the speed 60 m/s. It can be observed that, in the case of the active PID-ZN controller, the reduction of the car body's lateral displacement peak is approximately 63 % compared to passive suspension.

To calculate the Sperling ride comfort index (European Rail Research Institute 1993; Chen et al. 2005). The FFT plot is generated for a frequency range between 0 and 1000 Hz, as the human beings are most sensitive in the frequency range of 4–12.5 Hz. Ride comfort analysis has been performed for speeds ranging from 15 to 60 m/s.

The analysis has been performed on the system model to calculate the vertical acceleration of the system. FFT output is taken to get the peak acceleration frequency component. Comfort index for passive system has been presented in Table 4.

The maximum and minimum ISO Sperling Index values are respectively 3.17 and 2.03 for the rail vehicle speed respectively 15 and 60 m/s. These values respectively indicate "Strong, irregular, but still tolerable" and "Clearly noticeable" zones.

This means that the passengers are not much affected by the vibration as they are exposed to low level of vibrations for this type of irregularity. From Table 5, the

Table 5 Sperling's ride index evaluation for different vehicle velocities (active system)

Vehicle speed (m/s)	Sperling index (W_z)	Ride comfort evaluation
15	1.17	Just noticeable
30	1.54	Just noticeable
45	1.15	Just noticeable
60	1.03	Just noticeable

active PID-ZN controller keeps the passenger in a "just noticeable" level of comfort for all speed values.

6 Conclusion

Lateral control dynamic analysis has been carried out for a Railway Vehicle. A 17 degree of freedom model is used for the analysis. A lateral acceleration response at the car body has been calculated in the frequency domain. The Sperling Ride index has been calculated and presented for the above vehicle at different speeds. The calculated values of the Sperling index are found well in the satisfactory limits defined by the ISO 2631 standard which means that the passengers are not much affected by the vibration as they are exposed to low level of vibrations. It should be noticed that the control model was carried out to improve Wz index for all speeds.

References

Abood KHA, Khan RA (2011) The railway carriage simulation model to study the influence of vertical secondary suspension stiffness on ride comfort of railway carboy. J Mech Eng Sci 225:1349–1359

Chen H et al (2005) Application of constrained $H\infty$ control to active suspension systems on half-car models. Trans ASME J Dyn Syst Measure Control 127(3):345–354

Zhou R et al (2010) 9 DOF railway vehicle modeling and control for the integrated tilting bolster with active lateral secondary suspension. In: IEEE, UKACC international conference on systems technology control, vol 465, pp 1–6

Ang KH, Chong GCY, Li Y (2005) PID control system analysis, design, and technology. IEEE Trans Control Syst Technol 13(4):559–576

Dukkipati V, Amyot J (1988) Computer aided simulation in railway dynamics. Marcel Dekker, New York

Eski I, Yıldırım S (2009) Vibration control of vehicle active suspension system using a new robust neural network control system. Simul Model Pract Theory 17:778–793

European Rail Research Institute (1993) B153/RP21: application of ISO standard to railway vehicles comfort index N_{mv} comparaison with the ISO/SNCF comfort note and with the W_z

Kumar H (2006) Sujata: vertical dynamic analysis of a typical indian rail road vehicle. In Proceedings on computational mechanics and simulation, IIT, India, pp 8–10

Nejlaoui M et al (2013) Multiobjective robust design optimization of rail vehicle moving in short radius curved tracks based on the safety and comfort criteria. Simul Model Pract Theory 30:21–34

Pratt I (2002) Active suspension applied to railway trains. PhD thesis, Department of Electronic and Electrical Engineering, Loughborough University

Skarlatos D et al (2004) Railway fault diagnosis using a fuzzy logic method. Appl Acoust 65 (10):951–966

Vincent J (1999) Etude du concept de suspensions actives: applications aux voitures ferroviaires

Wolfgang A (2005) Practical control for engineers and technicians, 115–117

Zhang YW et al (2013) Riding comfort optimization of railway trains based on pseudo-excitation method and symplectic method. J Sound Vib 332:5255–5270